LASER INTERFEROMETER GRAVITATIONAL WAVE OBSERVATORY
-LIGO-
CALIFORNIA INSTITUTE OF TECHNOLOGY
MASSACHUSETTS INSTITUTE OF TECHNOLOGY

Technical Note	**LIGO-T0900128- v3*rev***	7/01/09rv

Scattered Light Loss from LIGO Arm Cavity Mirrors

William P. Kells

This is an internal working note
of the LIGO Project.

California Institute of Technology
LIGO Project – MS 51-33
Pasadena CA 91125
Phone (626) 395-2129
Fax (626) 304-9834
E-mail: info@ligo.caltech.edu

Massachusetts Institute of Technology
LIGO Project – MS 20B-145
Cambridge, MA 01239
Phone (617) 253-4824
Fax (617) 253-7014
E-mail: info@ligo.mit.edu

WWW: http://www.ligo.caltech.edu

File /home/Kells/documents/T9000xx.ps – printed September 20, 2004

I INTRODUCTION

For LIGO we are much interested in the fraction of incident [prescribed Gaussian mode beam] light lost ("scattered" out) from the mode when it is reflected from a mirror surface. Images of this light, from various non-specular view points, are by now familiar (figure 1). The apparent *statistical* homogeneity of the luminosity is striking which we adopt as a principle in our analysis. Guidance is given by the closely related theory of [statistically homogeneous] "laser speckle" scatter[1]. However nominally that theory applies to *rough* surfaces (surface point-point height variations $>\lambda_0$), in which case all incident light is scattered (no specular beam). For LIGO surfaces, residual surface "micro"-roughness is anticipated (via fabrication epoch metrology) to be shallow ($\ll\lambda_0$)[2]. In addition we know operationally that the loss fraction is $\ll 1$ with a specular mode accounting for essentially all the incident power. This suggests a perturbative analysis where the mean scatter field is of order the first [scaled dimensionless] moment of the inhomogeneity, that is σ/λ_0.

For single (*specimen*) surfaces only *inhomogeneities* scatter (*defined* as that differentiated from the specular *reflection*). Therefore loss cannot be uniformly distributed and a local "speckle" character (Fig. 1) is to be expected. Such generic character cannot inform on what the distribution in "size" (scattering amplitude) of the inhomogeneities is (given that they are not directly resolvable by accessible imaging). Distinguishing categories in the distribution is vital for LIGO since they likely arise from different phases of mirror fabrication. Micro-roughness inhomogeneities residual from substrate polishing are expected to be ~Gaussian distributed with very small, perturbative σ. Then outliers from this category (not necessarily perturbative) may be regarded as *defects* arising at some other, potentially improvable, stage of processing. Sufficiently high quality mirrors exhibit only "point" defects, that is not typically optically resolvable (<10μm) and so are sporadically (otherwise they could not be distinguished as outliers of a more pervasive distribution) distributed. Here we derive signatures of perturbative homogeneous micro-roughness scatter in order to distinguish (and quantify) any point defect component. Accumulated evidence (in situ scatter measurements as presented here; higher than anticipated total LIGO arm cavity losses; and laboratory surface scatter loss scans)[3] indicates that point defects (including surface contamination) strongly contribute to net mirror loss.

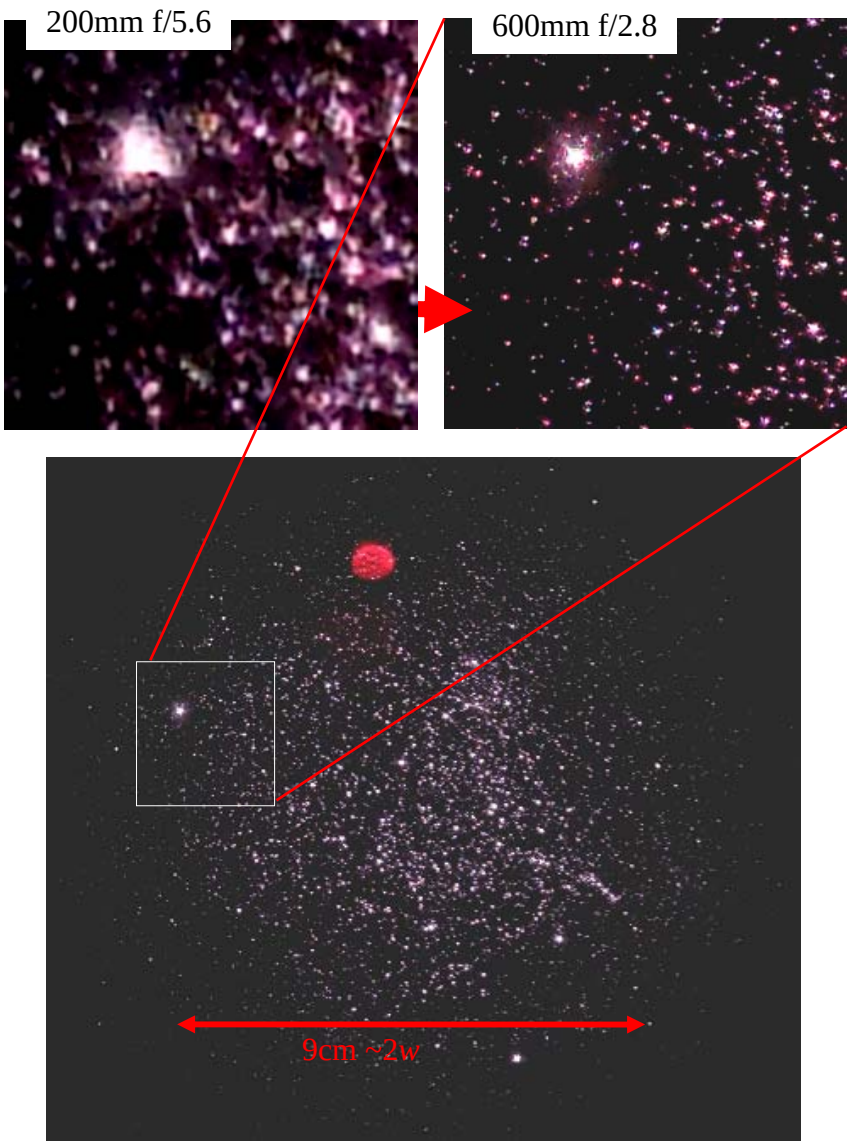

Figure 1. High resolution images of the beam spot on LIGO ETM mirror. The apparent "globular cluster" shape is due to the Gaussian surface illumination. It is clear that certain extreme bright points are flaws. Otherwise the "star" sizes are consistent with diffraction limited imaging optics. The view point used for this imaging is the highlighted in Fig. 3

II Connection to "laser speckle" scatter.

Under the assumption that residual distortions from the extreme mirror surface (polish+coating) regularity of interest (~ LIGO mirrors) are homogeneous in an ensemble mean sense we can analyze the statistical properties of coherent light scattered from specimens of the ensemble. The field of a finite (Gaussian width w) beam scattering from such specimens was developed[4], which we use as our starting point. Since the relevant surface area is finite (LxL~$4w^2$), it is convenient to approximate it as a matrix of NxN coherently scattering pixels (N sufficiently large that $L/N \rightarrow < \lambda_0$). Already in that primary analysis the "golden rule" net loss formula was re-derived (conditions of validity discussed):

$$P_{scatter} \approx P_0 \,|\, 4\pi\sigma_{eff} / \lambda_0 \,|^2 \qquad (1)$$

Features of this lumped loss will only be referred to. Instead here the main goal is to elucidate the intensity distribution, as illustrated in figure 1, using the same DFC beamlet, representation of the scatter field. The essential feature in describing the diffraction scatter in this way is that then it is formally analogous to the established statistical analysis of "laser speckle" scatter[1]. Therefore most canonical "speckle" characteristics may be reinterpreted for our situation. These give clean predictions for properties of data images (e.g. figure 1) dependent on the nature of the surface distortions.

First, summarize the essentials of speckle scatter theory[1]. The pixels which the reflecting ("scattering") surface is divided into are considered be of individually random height $h_{\mu,\nu}$ (over interval $\geq \pm\lambda_0$, hence *rough*) from a specular reference surface. Statistically it is vanishingly unlikely that any such specimen surface distortion would be isotropic. However *ensembles* of them are both isotropic and homogeneous. In this special, *completely* random case the specular reference surface shape (spherical, flat, etc) as well as the extent (L) of this rough distortion (as long as L> incident beam size) are irrelevant. Even the pixel size (L/N) is not crucial (needs not $\rightarrow <\lambda_0$) as long as a statistically sufficient number fill the illuminated area (or object Airy patch for imaging analysis, see below). The reflected field from such specimens at any distant observation point $\boldsymbol{r}$ is given as the sum over [~equal magnitude] random phasors representing each pixel[1,4]. The ensemble mean square of these sums (intensity when obliquity is separately factored in) is the same for any $\boldsymbol{r}$. Therefore there is no distinguishable *specular* reflection, and the incident power, $\mathbf{P}_0$, is all scattered with mean intensity $\mathbf{P}_0\cos\theta/\pi r^2$ (polar θ from incident, there being no azimuthal dependence in this *scalar* treatment). Of course, for any one specimen the intensity is distributed as randomly as the specimen pixels are.

The merit of analyzing in terms of a large number of randomly independent pixel/phasors is that the central limit theorem (CLT) may be invoked to predict likelihood distributions for physical quantities of interest for *likely* specimens (examples of which it is assumed we are always dealing with). For example the field amplitude distribution [over the ensemble] is Gaussian via the CLT. This implies that the intensity distribution is $\propto e^{-I/I_0} dI$ (I_0 being the mean given above), so that the most likely intensity at any point is zero. This describes the characteristic spatial intensity fluctuation of speckle (quantitatively confirmed experimentally).

The speckle "size" (specimen field autocorrelation width, taken to be identical to 2 point ensemble correlation) is also predicted. The correlation angle δθ between two far field points (**P-P′,** figure 2) is λ_0 / L so that the speckle "size" is~ $r\lambda_0 / L$ [5]. Note that this is the same as the Airy disc width of a constant amplitude illuminated aperture radius ~L/2 (a first Fresnel zone). The form of the speckle field may be thought of as a superposition of isotropically distributed such Airy disc amplitudes each of random phase. Also, speckle may be observed in telescopic (field lens, D and fl, normal to $\boldsymbol{r}$ at

any **P**/**P**′) images of the illuminated scattering surface. Such images must consist of intensity features no smaller than the Airy radius $\rho_A \sim f l\lambda_0 / D$, resolving only "object" (scattering surface) patches of radius $d_A/2 \sim r\lambda_0 / D >> L/N \sim \lambda_0$. Therefore adjacent patches are randomly different, and their adjacent image spots of randomly different intensity. Thus the image speckles are of mean size ρ_A(evidently the "stars" of Fig 1).

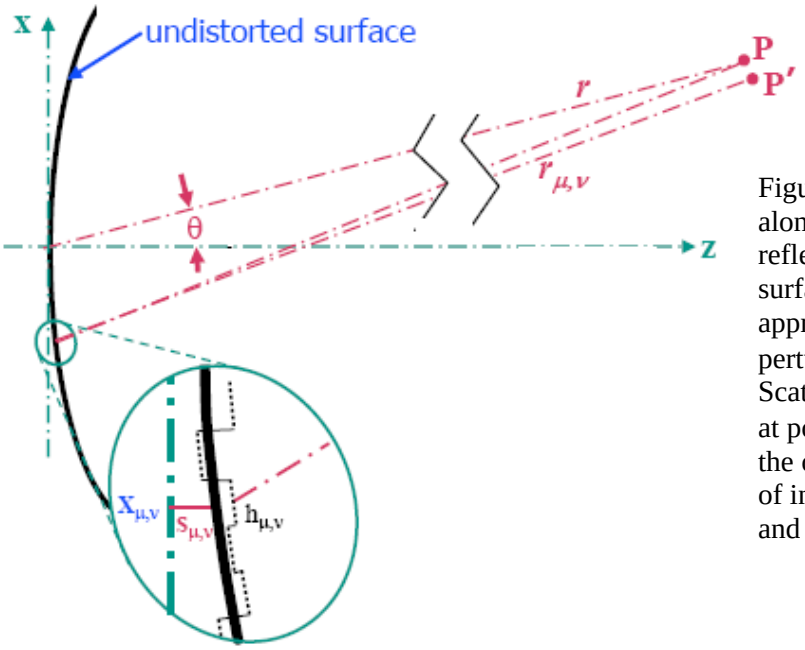

Figure 2. Beam incident along z axis) perfectly reflects from specular surface by distortion approximated by pixel perturbations $h_{\mu,\nu} << \lambda_0$. Scatter field is observed at points **P**(*r*), **P**′(*r*) w.r.t the origin (intersection of incident beam axis and undistorted surface).

III Differences with "laser speckle" scatter.

Although actual images (Fig. 1) and the plausibly random residual surface roughness of LIGO-like mirrors suggest a speckle analogy, three major differences make any direct application of the above results unclear. First, the distortion (pixel) height scale is far ($\ll \lambda_0$) from being rough[2], with, e.g. the conspicuous qualitative consequence that there is a dominant specular reflection. Second, although at least quasi-homogeneous, it is known that otherwise flawless precision polishing results in a fractal power spectrum of residual surface distortions[3,6]. This means that the scatter (even in the ensemble average) can only be *azimuthally* isotropic, whereas completely random pixels would scatter, in the mean, uniformly (Lambertian) in all directions. That is, there are strong long range correlations amongst the $h_{\mu,\nu}$ of any realistic polished surface even if regarded as being homogeneous. Third, closely related to this, is the fact that a true fractal homogeneous distortion ensemble is not possible for the finite specimen mirrors actually fabricated. There is always some surface scale at which the homogeneity and isotropy break down[4]. Some results e.g. total loss (1) which include scattering from all scales will remain intrinsically uncertain in any statistical analysis[7].

IV Perturbative beamlet speckle scatter.

Here perturbative random ensemble description of micro-roughness (e.g. LIGO-like) scattering is developed in analogy to the canonical speckle theory, naturally incorporating these differences. Fresnel-Kirchhoff diffraction, expressed to $\mathcal{O}(\mathrm{h}_{\mu,\nu}/\lambda_0)$ as discreet sums over monochromatic radiation from the surface pixels, gives the [far] **P**(*r*) field. For LIGO-like parameters (*w*/ROC<<1, $|\mathrm{h}_{\mu,\nu}|/\lambda_0 \ll 1$), each DFC of the pixel array (N^2 over L^2) distortion becomes the coefficient $\tilde{\mathrm{h}}_{\mathrm{m,n}}$ of a diffracted Gaussian *beamlet* propagating in the grating direction $\hat{\mathbf{k}}_{m,n}$ corresponding to that DFC. This is an accurate representation assuming 1, neglect of aberration terms $\mathcal{O}(w/ROC)^2$; 2, first order in the perturbation $\mathcal{O}(\mathrm{h}/\lambda_0)$; 3, scalar wave approximation; and 4, paraxial description of the beamlets[4]. This decomposition allows for arbitrary beamlet [magnitude] spectrum (within the constraint of assumption 2. and Parseval's condition), accommodating any presumed (e.g. fractal) distortion and anisotropic scatter intensities. Restriction to *homogeneous* distortion ensembles requires these coefficients be of mutual random *phase*. This *phase* randomness provides the direct analogy to pixel *height* randomness in canonical speckle theory.

The $\tilde{\mathrm{h}}_{0,0}$ coefficient DFC represents the specular diffraction at θ=0 which we avoid by observing only at large angles (θ >.017 Rad, or $\tilde{\mathrm{h}}_{\mathrm{m,n}}$ where $\sqrt{\mathrm{n}^2+\mathrm{m}^2} > 1800$). This practically avoids ambiguous treatment in regions influenced by the specular beam and surface inhomogeneities (large surface scale: 3^{d} caveat above). Figure 1 is at a typical accessible observation point, with θ_{Obs} =0.16 and *w*<<*r*~5m<<r_{Ray}. Thus any beamlet subtends dθ<*w*/r<<θ so that only a small fraction dk/k of the DFC spectrum contributes at this point. For reasonably smooth ensemble spectra we can then approximate contributing $|\tilde{\mathrm{h}}_{\mathrm{m,n}}|$ to be constant. On the other hand this contributing band of DFCs all interfere with random phases and are sufficiently numerous ($\sim(4w^2/\lambda r)^2 \sim 10^6$) to invoke the same statistical argument used for canonical speckle. The *mean* intensity in direction θ_{Obs} (or **m,n**) is just proportional to the intensity $\left|\tilde{\mathrm{h}}_{\mathrm{m,n}}\right|^2$ of the central beamlet, and distributed with exponential probability (same as for speckle). Similarly the *mean* size of the speckle is given by the angle (**P-P′**) over which a particular band of beamlets coheres $\sim \lambda_0/2w$ [8]. In this discussion the "*w*" used is strictly the beamlet Gaussian width at *r*. However for Fig.1 (and all directly accessible observation points) *r* <<r_{Ray} so that there is negligible **O-P** variation in *w*.

This result may be used to resolve a crucial experimental question. The original (and by now considerable) data measuring the LIGO arm cavity mirror scatter consisted of monitoring the net power impinging on a PD (area or collecting lens a^2) placed at **P** (

Fig. 3,normal to ***r***)[3]. Practical constraints require this PD **P** to remain fixed, so there has been no attempt to survey the PD sampled field to establish [local] mean I_0. However it has been presumed that these PD measurements are accurately proportional to this *mean* scatter field intensity for their θ location. Since we observe only single specimen, this can only be valid if a is sufficiently large. Now we understand the criteria for accurate mean PD sampling to be that "statistically many speckles fall within PD collection area" or > $(aw/\lambda r)^2 \sim 10^3$ for the above case[9]. This criterion for uniform PD response is essentially the same as described above for [rough surface] speckle, the only difference being in the definition of "*w*"[5]. Therefore any [additional] scatter contribution from rough "point" defects would be also be uniformly sampled as long as there are statistically many of them within the mirror beam spot.

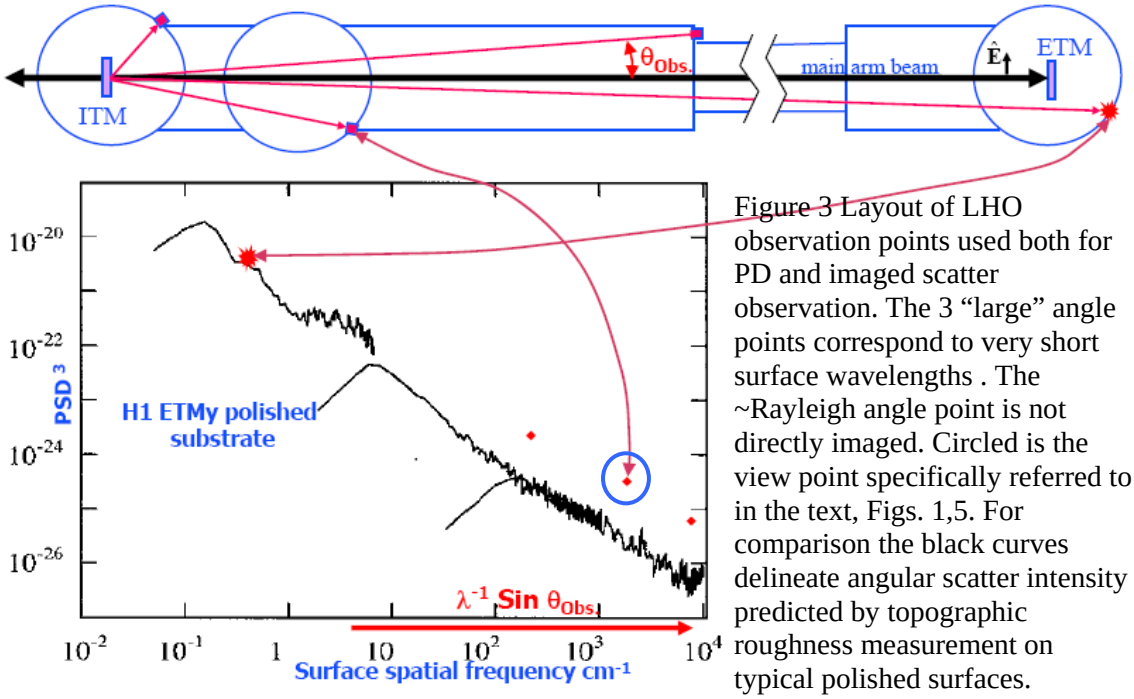

Figure 3 Layout of LHO observation points used both for PD and imaged scatter observation. The 3 "large" angle points correspond to very short surface wavelengths . The ~Rayleigh angle point is not directly imaged. Circled is the view point specifically referred to in the text, Figs. 1,5. For comparison the black curves delineate angular scatter intensity predicted by topographic roughness measurement on typical polished surfaces.

V Imaged micro-roughness scatter.

Qualitatively, the circumstances and appearance of images (Fig. 1) of optic surfaces at non-specular θ_{Obs} have striking "laser speckle" resemblance. To quantify this, first recall that any imaging system cannot display features finer than the Airy disc ($2\rho_A = 1.2\lambda_0 f\#$, "diffraction limited" for telescope aperture D, f# =[fl/D]). This corresponds to an Airy "patch" (diameter $d_A = 1.2r\lambda_0/D$)[Y] on the object outside of which pixels cannot contribute significantly to the image Airy disc amplitude. For all imaging configurations investigated in LIGO, $d_A > 0.1$mm so that most isolated "point" defects are unresolved, appearing as Airy "stars" of Fig.1. The field of any particular "$\mathbf{d_A^2}$" patch may be expressed as a sum of the field amplitudes from each surface pixel **(μ,ν)** it contains:

$$\propto \frac{qE_o(\mathbf{x}_{\mu,\nu})e^{i2\pi \mathrm{h}_{\mu,\nu}}}{r_{\mu,\nu}} e^{i2\pi|\mathbf{x}_{\mu,\nu}+(\mathbf{s}_{\mu,\nu}+\mathrm{h}_{\mu,\nu})\hat{\mathbf{e}}_z+\mathbf{r}|/\lambda_0} \qquad (\boldsymbol{\mu}, \boldsymbol{\nu}) \in \mathbf{d}_{\mathrm{A}}^2 \tag{2}$$

where we follow closely the derivation of [4] (Eqns.12-16). Since PD detection (section **IV**) involves superposition from *all* surface pixels it was necessary to represent the sums over (2) as global beamlets. Here the restriction to pixels only *within* $\mathbf{d}_{\mathrm{A}}^2$ allows simplification of the form of sums over (2). For imaging to be quantitatively interesting we want to resolve surface features $d_A << w$. The Gaussian optics of the undistorted cavity surfaces is such that $w \geq \sqrt{\lambda_0 ROC}$. Therefore the local undistorted surface sag across d_A is $<<\lambda_0$, itself perturbative. Further, the condition $d_A << w$ allows $E_0(\mathbf{x}_{\mu,\nu})$ of (2) to be approximated as constant across $\mathbf{d}_{\mathrm{A}}^2$. Considering now only micro-roughness, the patch contains no rough ($h_{\mu,\nu} \sim \lambda_0$) defects, allowing the sum of these pixel contributions to the field "at" (or within, noting that this restriction assumes exact focusing on the imaging plane, but see next section **V**2) $\boldsymbol{\rho}_{\mathrm{A}}^2$ to be written as:

$$\mathrm{C}_\theta \frac{E_o(\mathbf{d}_{\mathrm{A}}^2)}{|\mathbf{x}_{\mathbf{d}_{\mathrm{A}}^2}+\mathbf{r}|} \sum_{\mu,\nu \in \mathbf{d}_{\mathrm{A}}^2} (\lambda_0 + \mathrm{h}_{\mu,\nu} + \delta \mathrm{s}_{\mu,\nu}) e^{i2\pi|\mathbf{x}_{\mu,\nu}+\mathbf{s}_{\mu,\nu}+\mathbf{r}|/\lambda_0}$$

$$\mathrm{C}_\theta \equiv \frac{i2\pi(1+\cos\theta)\mathrm{L}^2}{\lambda_0 \cos\theta N^2} \tag{3}$$

Where $\delta s_{\mu,\nu}$ is the local sag w.r.t. a mean tangent plane in $\mathbf{d}_{\mathrm{A}}^2$. Proceeding as in [3], the specular ($\sim\lambda_0$) term is ignored and perturbative terms (h and δs) are represented by DFCs:

$$\mathrm{C}_\theta \frac{E_o(\mathbf{d}_{\mathrm{A}}^2)}{|\mathbf{x}_{\mathbf{d}_{\mathrm{A}}^2}+\mathbf{r}|} (\tilde{\mathrm{h}}_{m,n} + \widetilde{\delta \mathrm{s}}_{m,n}) e^{i2\pi|\mathbf{r}_{\mathbf{d}_{\mathrm{A}}^2}|/\lambda_0} \sum_{\mu,\nu \in \mathbf{d}_{\mathrm{A}}^2} e^{i(\hat{\mathbf{k}}_{\mathrm{m,n}} - \hat{\mathbf{k}}_\theta)(\boldsymbol{\mu},\boldsymbol{\nu})} \tag{4}$$

where $|\mathbf{r}_{\mathbf{d}_{\mathrm{A}}^2}|$ is the local distance to the observation point and $\hat{\mathbf{k}}_\theta \approx 2\pi \hat{\mathbf{r}} \mathbf{x}_{\mu,\nu} / \lambda_0 \equiv 2\pi \sin\theta(\boldsymbol{\mu}, \mathbf{0})\mathrm{L}/\mathrm{N}\lambda_0$ is the "grating" directional vector at the [polar] observation point angle θ_{Obs}. Since $\delta s_{m,n}$ represents the undistorted locally nearly flat surface shape, all its DFCs are negligible at θ_{Obs} of interest ($>>\lambda/2w$). The sum in (4) is ~zero unless $|\hat{\mathbf{k}}_\theta - \hat{\mathbf{k}}_{m,n}| < \lambda_0 / d_A$, so that only a narrow band, **Δ(n,m),**

where $|\tilde{h}_{m,n}| \approx \text{Const}$, contributes to $\boldsymbol{\rho}_A^2$: Summing over all such non-negligible components gives the net amplitude at $\boldsymbol{\rho}_A^2$:

$$\approx C_\theta \frac{E_o(\mathbf{d}_A^2)}{|\mathbf{x}_{\mathbf{d}_A^2} + \mathbf{r}|} |\tilde{h}_{m,n}| e^{i2\pi|\mathbf{r}_{\mathbf{d}_A^2}|/\lambda_0} N_{\mathbf{d}_A^2} \sum_{\Delta(\mathbf{m},\mathbf{n})} e^{i\varphi_{m,n}} \qquad (5)$$

where the [ensemble] random phases, necessary for homogeneity, of each DFC are displayed and $N_{\mathbf{d}_A^2}$ are the number of pixels within $\mathbf{d}_A^2$. For given camera view point and settings all factors in (5) except the sum are practically constant or vary smoothly (E_0 and $\mathbf{r}_{\mathbf{d}_A^2}$ phase) across the beam image. These determine systematic position *mean* brightness within the image. Locally however, at each $\boldsymbol{\rho}_A^2$ the sum is Gaussian random since a large number, $\mathcal{O}(L/d_A)^2 \geq 10^4$ (analyzed images, e.g. Fig. 1,5) **(m,n),** contribute[11,12]. These conditions imply locally the same (exponential) image intensity statistics as held for canonical rough speckle. We conclude that small neighborhoods in diffraction limited focused micro-roughness scatter images have the same exponential (mean $\propto |\tilde{h}_{\Delta(m,n)}|^2$) as equivalently imaged canonical speckle fields.

Such "imaged" speckle (rough or micro) is not a true image since the actual surface (except global, geometrical features) is entirely unresolved. One manifestation of this is that image detail cross correlation with vanish between views differing by more than a certain $\delta\theta_{Obs}$. Follow the image of the same patch $\mathbf{d}_A^2$ as the camera observation point rotates to $\theta_{Obs} \pm \delta\theta$. According to the criteria leading to (5) only **(m,n)** such that $|\hat{\mathbf{k}}_{\theta\pm\delta\theta} - \hat{\mathbf{k}}_{m,n}| < \lambda_0/d_A$ will contribute, and these bands will contain all different components (of randomly different phase) if $\delta\theta > \lambda_0/d_A$. Thus there is a $\delta\theta$ correlation angle (see **VI** 2) outside of which images of the *same specimen* beam spot will appear statistically similar but have vanishing *same* surface point cross-correlation. Isolated and sufficiently bright "point" defects will have invariant image Airy discs since their DFC phases are completely correlated (prescribing their position, see **VI** 3).

2. Correlation width (speckle size) in image: van Cittert-Zernike theorem.

Although the local image Airy diffraction point statistics (across the ensemble) are plausibly Gaussian via the CLT, it is not as simple to conclude that the correlation width (again ensemble average) within the scatter image is $\sim\rho_A$. Correctly accounting for the DFCs and phasing contributing to $\boldsymbol{\rho}_{A'}^2$ adjacent to a fiducial $\boldsymbol{\rho}_A^2$ involves delicate calculation. For example, consider the image of a single pixel source (at focal distance ~fl for source to lens distance $r \to \infty$). The image field is a single Airy distribution. This source may equivalently be considered as a coherent spherical wave, practically plane as it approaches the imaging lens from sufficient [telescopic]

distance. The Debeye/Lommel theory of this wave apertured by lens (D,fl) indeed gives the Airy distribution at plane $\boldsymbol{f}(r \to \infty)$[13]. However this impinging wave front (now at non-telescopic distance r' may be considered (via Huygen's principle) as a uniform density plane of [coherent] point sources *each* of which contributes its own Airy distribution but at a unique transverse point in the $\boldsymbol{f}(r')$ plane. It can be shown that the superposition of this plane of ostensibly distinct Airy patterns is exactly a single one at $\boldsymbol{f}$=fl[14].

Instead of such a delicate explicit calculation superpimposing all imaged μ-roughness point sources ($\propto E_0(\mu,\nu)h_{\mu,\nu}/\lambda$) to calculate the image plane field strength correlation, we use the fact that, appropriately restricted, the van Cittert-Zernike (vCZ) theorem is applicable[15]. This result nominally applies to uniform, *incoherent* (and therefore non-monochromatic) sources[16]. Our strictly coherent specimen source can be regarded as incoherent by considering an appropriate statistical ensemble of statistically equivalent specimens. Our already adopted *homogeneous* ensemble over all $\tilde{h}_{m,n}$ phases is uniform and otherwise appropriate[YY]. Of course the scattering source from this surface ensemble is not uniform since it is Gaussian beam illuminated. However it may be shown that for this special, smooth non-uniformity vCZ similarly holds[5].

The vCZ results describe the quasi-monochromatic field spatial coherence at an image plane. For our monochromatic ensemble analogy this is equivalent to the image plane ensemble averaged spatial correlation. Perhaps not so surprisingly the predicted image spatial coherence function is exactly the Airy [field] distribution function for [circular] lens aperture D and imaging distance $\boldsymbol{f}$. Besides source incoherence and uniformity, the vCZ results require only that the source extent (~2w) be [much] larger than d_A which, we have seen, is always the regime of interest at LIGO. More surprisingly the correlation at $\boldsymbol{f}$ is only dependent on ~λ $\boldsymbol{f}$/D and not on $\boldsymbol{f}$ being the geometrical focus $\boldsymbol{f}(r)$ for the source. That is, there is no plane where speckle is "in focus" [15]. The apparent imaged size of the perturbative μ-R scatter (as long as it has phase ambiguity inherent in the considered ensemble) *scales* $\propto \boldsymbol{f}$ but otherwise is determined only by the pupil aperture. In practice we do "focus" the camera lens on unambiguous surface features (inhomogeneous flaws, edges, etc.) which, at our working distances, constrains $\boldsymbol{f}(r)$~fl so that the speckle in beam spot images (Fig. 1) has "size" essentially that of the camera [lens] Airy resolution 1.2λf#.

VI Predictions for and analysis of images.

During the course of LIGO(Hanford) commissioning a few images[3,17] were taken under sufficiently controlled circumstances to apply simple quantitative processing techniques. For these the perturbative speckle interpretation (last section) should well apply, implying several predictions for images as a function of camera parameters (θ_{Obs}, r, camera f# and fl). Reliable data was limited to observations at a single r (~5-6m), however there was some flexibility on θ_{Obs} (within view port aperture; opposite beam tube sides). The goal of this quantitative image analysis is to distinguish any

violation of these micro-roughness regime predictions indicating significant (w.r.t. loss) point defect scattering. Indications of excess cavity loss (operational and corroborated by TIS mirror surface scans) plus the large angle point-like PD data excess in Fig. 3 motivates this pursuit[18].

1. **Camera f# dependence.**

First we consider fixed θ_{Obs} images (leaving only camera f#, fl variable). The quantitative technique is to histogram the CCD pixel values ("intensities") as in figure 5. In all cases the CCD "pixel scale" is $<<\rho_A$. Data fields are cropped from full beam images to correspond ~uniform beam illumination ($|E_o(\mathbf{d}_A^2)| \approx Const.$), yet still contain a large statistical sample of speckle (*crop width*$>>\rho_A$). Under these circumstances, CCD pixel intensity values imaging homogeneous micro-roughness will mimic the probability distribution for $\boldsymbol{\rho}_A^2$ derived above: $dn(I) \propto N_{Tot} e^{-I/\langle I \rangle} dI$, with mean image intensity:

$$\langle I \rangle_{\text{camera Obs. } \theta} \propto P_0 \left\langle |\tilde{h}_{m,n}|^2 \right\rangle_{(\mathbf{m},\mathbf{n}) \in \mathbf{k}_{Obs}} (f_{\#})^{-2} \tag{6}$$

Therefore, as long as a significant sample of speckles are resolved in the cropped image, the distribution of intensity depends *only* on f#. This allows close comparison of images where f# is varied via lens aperture setting (same fl lens). In comparison, "point" defects are not resolved so that their apparent ($\boldsymbol{\rho}_A^2$ peak) intensity is:

$$I_{\text{Peak}} \propto P_0 \left(\frac{fl}{r} \right)^2 (f_{\#})^{-4} \tag{7}$$

According to (6-7) any point component may be discriminated by comparing image pixel histograms at various f#. This is schematized in figure 4, making clear that any intense image points eventually loose contrast against a "sea" of background speckle as $f\# \to \infty$[11]. Sufficiently low resolution (high f#) images were found to follow the exponential distribution within statistical resolution[3]. Figure 5 analyzes a central crop of the same image shown in Fig 1, representing our highest resolution data. A

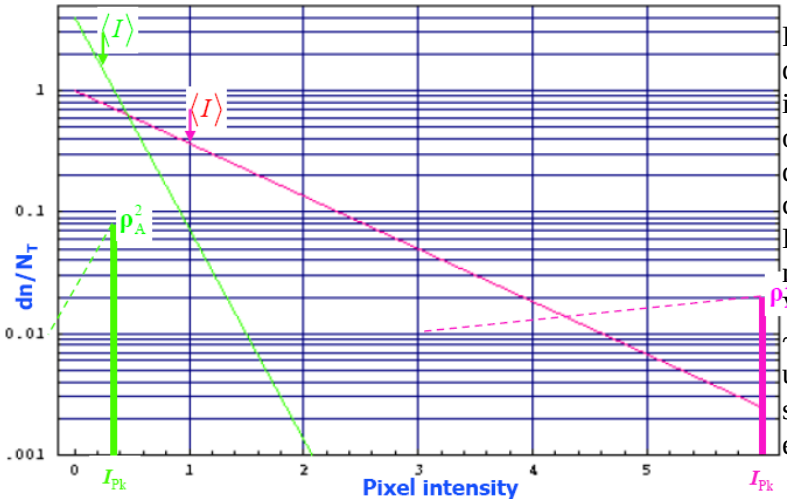

Figure 4. Comparison of distributions of CCD pixel intensities for same imaged object area. Pink and green distributions differ only in camera f# value (f# =2f#). Exp[-*I*/<*I*>] lines represent micro-roughness speckle. Vertical bars represent ~peak bins from isolated unresolved point defect scatter. $f\# \to 0$ greatly enhances the point contrast

dominant point component is indeed resolved. However since the observation point $|\hat{\mathbf{k}}_{m,n}|$value "angle" for this image is large, micro-roughness contributes with weight $\propto |\tilde{h}_{n,m}|^2 / |\mathbf{k}|$ (<<1 at large angle points in Fig. 3) relative to ~isotropic point scatter. Most of the surface spectrum (e.g. small $|\hat{\mathbf{k}}_{m,n}|$,* point in Fig.3) is, unfortunately, not accessible to imaging, is evidently dominated by micro-roughness. Thus this current level of image analysis does not have sufficient angular (spectral) coverage to determine the point defect *loss* fraction. However, these large angle observations are ideal diagnostics of point defects yielding high contrast images of their density and distribution.

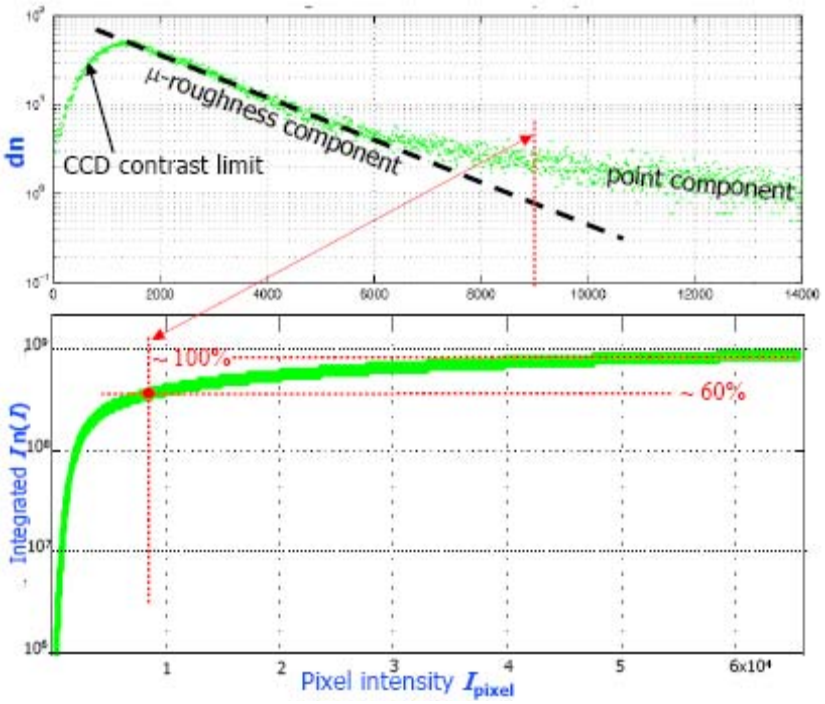

Figure 5 High resolution histogram (top) of central crop of Fig. 1 image (f#2.8). CCD/readout limitations roll u-rough exponential off at low intensity. Intensity weighted integrated (bottom) histogram used to evaluate point component as ~90% of total scattered light at this θ_{Obs}. The departure from exponential at low brightness is due to inevitable contamination by some independent speckle (or noise) source[19].

2. Camera view angle dependence.

Second, we investigate how images differing only in observation angle are correlated. Here we ignore geometrical angular dependent aberrations (such as obliquity and foreshortening astigmatic effects which are, in any case, deterministically removable from correlations), and assume the incident beam position and intensity is constant (scattering source invariant). This implies limiting to comparisons over small angles, consistent with the correlation (5) of angles $\delta\theta_{Obs} < \lambda_0 / d_A$ for pure (homogeneous) micro-roughness images scatter. But this corresponds to a lateral shift in camera position, $r\delta\theta_{Obs} < D_{lens}$. That is, shifting the camera laterally by greater than one aperture diameter should yield locally randomly different image speckle patterns[12]. LIGO observation ports accommodate studying this since their clear diameters are several times that of typical used camera apertures. In existent images corresponding to θ_{Obs} Fig1,3,5 significant image correlation is apparent (but not yet systematically quantified) beyond this limit. This is consistent with the significant point component found in Fig. 5 (and corresponding points in Fig. 3). Since the images are in stable digital format it would be straightforward to systematically (say as a function of $\delta\theta$) calculate intrinsic (local) cross correlations, normalizing out extraneous DOFs (exposure/illumination changes; view point aberrations, registration, etc.). Given the anticipated steep spectrum for $|\tilde{h}_{m,n}|$ (Fig.3) substantial de-correlation would be expected over images at very small θ_{Obs}. However this regime is practically inaccessible to the LIGO configuration (Fig. 3).

Fig. 3 indicates a strong *mean* scatter intensity dependence on θ_{Obs}. Since sporadic "point" defects are expected to scatter approximately isotropically, this data indicates that a defect component does not saturate the mean (loss)[20], though it could[2]. With imaging of high enough resolution (e.g. Fig. 5) to distinguish a sporadic non-Gaussian component a strong difference in certain speckles image brightness with θ_{Obs} should be readily apparent. Image pairs (and image analysis algorithms) optimized (i.e. *only* θ_{Obs} changed) in this vein have not yet been pursued. Close archival pairings indicate the expected pixel histogram behavior (i.e. increased relative "point component", per Fig. 5, at increased θ_{Obs}).

3. Image defocusing invariance.

For incoherent light we intuitively appreciate that an entirely uniformly featureless (color as well as brightness) object will have no distinct focal plane regardless of its distance, *r*. Zernike demonstrated (section **V**2) that not only such *first order* properties (*mean* intensity) are focus invariant, but so too are *second order* ones (coherence correlation). Any inhomogeneities on the object (e.g. its

edge, or a bright point within) will obviously be sharply focusable, and (not so obviously) concomitantly violate coherence correlation invariance[15]. For the LIGO coherent illumination case, ensemble averaged image properties analogously depend on the source object homogeneity. Here the [local] "brightness" (beam illumination) is given as uniform. Therefore any inhomogeneities can only be introduced in defining the ensemble. In this sense our previous definition of random DFC phases assures homogeneity. This corresponds to each *specimen* of the ensemble being statistically indistinguishable. Certainly fluctuations may occur amongst these (with Gaussian outlier pixel groups $h_{\mu,\nu}$ of (2,3) which would image as particularly bright fluctuations). As long as our particular specimens (mirrors) are well described as members of the Gaussian distribution there will be no ensemble definable "in focus" image plane. However it is quite possible for a given surface pixel to be *assigned* $h'_{\mu',\nu'} \gg \sigma_{h,ensemble}$. If this local feature is kept over the ensemble then it will emerge as a legitimate inhomogeneity (cannot be described as any spectrum of DFCs with ensemble random phases). Any specimen containing it would statistically be considered a [far] outlier from the Gaussian distribution of typical images. Thus it is only in this *non-Gaussian* sense that defects [pixels, or clusters] may be distinguished as inhomogeneities. There is no succinct qualitative way to distinguish individual "defects" from mere local fluctuations in the surface μ-R.

Consider then the image of one such non-Gaussian pixel height "defect". Its height $h'_{\mu',\nu'}$ need only be a few $\sigma_{h,ensemble}$ to be extremely unlikely. Thus the particular mirror surface containing it cannot be legitimately modeled by a *homogeneous* ensemble of specimens characterized by σ_h. Only ensembles of specimens which retain an average non-Gaussian value at $(\boldsymbol{\mu}',\boldsymbol{\nu}')$ are physically legitimate. This ensemble will then be *in*-homogeneous and violate the vCZ image invariance. The image at distance $\boldsymbol{f}(r)$, i.e. exact focus for mirror surface at r, will have one Airy pattern (the image of that object patch $\mathbf{d}_{\mathbf{A}}^{\mathbf{2}}$ containing $h'_{\mu',\nu'}$) much brighter than the surrounding speckle (mean brightness $\propto \sigma_h^2$ of the ensemble). Of course the relative brightness (w.r.t. the mean surrounding speckle intensity) will depend on dilution (number $N_{\mathbf{d}_{\mathbf{A}}^{\mathbf{2}}}$ of Gaussian(σ_h) distributed pixels as discussed above,**VI**1) determined entirely by camera resolution. To the extent the brightness of this one Airy pattern is dominant it will defocus as the standard Lommel focal pattern[13]. Note that the spatial size of the intensity fluctuations in *any* image plane will remain the vCZ (homogeneous) value. However their contrast will vary from ~1 (far from the geometrical edge of the Lommel spot) to ~zero(within the Lommel spot as long as its mean intensity is not so defocused as to approach the homogeneous speckle intensity).

Generally we are interested in large numbers of non-Gaussian "defects" randomly distributed over the beam spot illuminated surface. In a coarse enough grained sense these may be regarded as homogeneous. If such a coarse grained description of any actual specimen allows adequate physical description of the surface then it

is legitimate to rely on the homogeneous ensemble of these specimens as a correct model. The coarse graining at which randomly distributed defects are not distinguishably in-homogeneous is when several (on average) occupy each grain area. That is, when their mean separation is $<d_A$ the defect distribution itself will scatter such that its image will be speckle with the same statistical character derived for micro-roughness. Phenomenologically then, focusability is not only a property of the source surface topography, but is convoluted with the imaging system resolution. The focus invariance of speckle had not been appreciated at the time of existent image studies (nominally all "in focus")[21]. It is clear from all other data (Fig. 1,3,5) that non-Gaussian points are a significant scatter component and have been resolved. This is consistent with the [anecdotal] fact that typical beam spot photography appears to have a very sharp focus. Archival examination of images with inadvertent defocus indicates a background component that is indeed invariant.

VII REFERENCES

1. J. Goodman, in Laser Speckle and Related Phenomena, Topics in Applied Physics Vol. 9, 2nd Ed. Springer, 1984. For a much more comprehensive and recent treatment, extensively referenced: *Speckle Phenomena in Optics*, J. Goodman, Roberts & Co, 2007.

2. On small scales, $\leq$ mm, polished surfaces with random rms roughness $\ll$ nm can be achieved. Then on long scales (up to the substrate diameter) systematic distortions ("aberrations") can also be held to $\leq$ nm amplitudes. On the other hand any process will have some [random] occurrence of flaws, typically "point" (in experience $\mathcal{O}$(pixel $\approx \lambda_0$) width) defects. Their local $h_{\mu,\nu}$ surface height distortion is either not perturbative ($|h_{\mu,\nu}| / \lambda_0 \geq 1$), or at least far larger than the rms roughness. It is only supposed that the ensemble of such defects contributes insignificantly to loss. If predominantly non-perturbative, defects could predominately scatter in a Mie regime (power scattered $\propto area \sim |h_{\mu,\nu}|^2$) dominating the net surface loss and yet insignificantly contributing to the net surface rms. This is to be tested against the statistical predictions from random micro-roughness alone.

3. W. Kells, LIGO-G080078, G070423, and G0900467-v2. Note that *indirect* measurement of scatter intensity was also inferred at one extremely small $\theta \sim \theta_{Ray}$ (V. Frolov,et al, LLO i-log, 2006). Indeed the scatter intensity in this regime (observed similar for all 3 LIGO interferometers) has strong local anisotropy, making an interpretation of mean I_θ highly uncertain.

4. W. Kells, LIGO-T070310-v1.

5. The ensemble averaged treatment of this correlation is exactly treated in Goodman's book [1] for the case of *uniform* illumination. Presumably an exact result for *Gaussian* illumination can be similarly found. However Zernike's treatment[15] of partial coherence in the far field is easily adopted for this. His result for a *uniform*, radius *w* source (i.e. coherence spreading as an Airy pattern of disc radius $0.6\lambda r/w$) becomes, if Gaussian(w) intensity illuminated, coherence spreading as a Gaussian, radius $\sqrt{2}\lambda r/\pi w$.

6. E. Church, P. Takacs, (and Leonard, SPIE Vol 1165); Handbook of Optics, Vol I; and SPIE Vol. 645.

7. Equation (1) is a clear example, attempting to express loss as a function of any σ^2, a *statistical* measure of the surface roughness. The general problem with exactly doing so was emphasized in reference 4. For fractal like surface structure (even if random and homogeneous) σ^2 has no fixed value but varies with L, typically diverging as $L \to \infty$. The natural L~(incident beam width) can be approximately adopted to define a σ^2_{Leff} however this is still ambiguous since diffraction (scatter field amplitude) is over [weighted] Fourier components of the roughness. No abrupt truncation of components (L^{-1}_{eff}) is equivalent. It is sometimes proposed that an "incident beam intensity (e.g. Gaussian) weighted σ^2_h" is the correct quantity to use in (1). This leaves just as ill-defined the sampling prescription for local measure of σ^2_h. Practically the concept is useful only for better predicting loss for characteristically *inhomogeneous* surfaces. The role the homogeneity constraint on ensemble results has been considered in E. Wolf and H. Carter, Opt. Comm. **13**, 205, and JOSA **67**, 785.

8. Here we use the identity that, as $N \to \infty$, $\sum_{n=0}^{N} e^{i\varphi_n}$ and $\sum_{n=0}^{N} e^{i\varphi_n} e^{i2\pi n/N}$ are completely uncorrelated for random φ_n.

9. The PDs (or their collection lens) were selected before this criteria was appreciated. It is fortuitous that the combination of PDs and observation points has been consistent with uniform scatter loss sampling. However the worst case sampling has been $n_{speckle} \le 100$, and this only because relatively large area PDs (> mm^2) have been used.

10. Strictly the central Airy disc depends on the exact focal distance $\boldsymbol{f}(r)$ and only $\boldsymbol{f}(\infty)$=fl. For all LIGO relevant situations r>>fl, so that ρ_A is well approximated by its "telescopic" value. However, the Airy "patch" ,d_A, is independent of this approximation.

11. Eventually, as f# increases the entire image becomes one, unresolved, Airy disc and (6) breaks down (as it must eventually go as $\sim r^{-2}$). This indicates that any distinction between micro-roughness and point scattering perturbations ceases to have meaning. Distinguishing point defects depends on their scattering amplitude dominating the net contribution to some $\boldsymbol{\rho}_{\mathbf{A}}^{\mathbf{2}}$. This contrast diminishes as the relative contribution of micro-roughness increases in proportion to $\mathbf{d}_{\mathbf{A}}^{\mathbf{2}}$. Even with no such competing micro-roughness any statistically significant N_{point} distributed on the surface will appear indistinguishable from speckle as $f\# \to \infty$ since the "isolated" points will begin interfering.

12. Given a fixed LxL discreet grid it would seem that $\mathcal{O}(L/d_A) \gg 1$ would break down. However, physically, over a realistic ensemble the field must retain the same random features as $r, d_A \to \infty$. Although fixed $L \geq 2w$ are sufficient to describe the net scatter (loss), the fixed grid pattern leaves non-random artifacts in the DFC description of the field. This can always be removed (to any far field angular scale) by formally employing a statistically equivalent surface with $L \to \infty$. This ensures $\mathcal{O}(L/d_A) \gg 1$ at any *r*, with Gaussian random field distribution. Similarly the de-correlation of image speckle upon lateral camera position shift $r\delta\theta$ >D cannot remain valid as D is reduced to a "pinhole" (<< far field un-imaged speckle width $\sim r\lambda_0 / 4w$). The break down in this "pinhole" limit entails the entire beam image coalescing into a single Airy disc with no correlatable structure.

13. *Optics*, Born and Wolf, section 8.8 (7^{th} Ed.).

14. Have worked this out exactly in terms of Fresnel integral over Airy patterns for every point in source plane.

15. F. Zernike, Physica **5**, 785 (1938) The elegantly simple original description by Zernike of this invariance is notationally confusing. The full qualitative extent of the result is brought out in Born & Wolf section 10.6.1 (7^{th} Ed.). The quantitative relation that the coherence/correlation width at the imaging plane is $\propto \boldsymbol{f}$ depends on the optical train being paraxial, e.g. that $\boldsymbol{f}$>D. It is clear that as $\boldsymbol{f} \to 0$ the coherence is determined by *w* (and *r*) not D at all.

16. The original work on optical coherence (e.g. [15]), all done before the Laser and observation of speckle, pertained to non-monochromatic light, so that [extended] sources were defacto incoherent. Although Born and Wolf mention the equivalence of this incoherence to that over monochromatic ensembles (e.g. section 10.4.2), Goodman (*Statistical Optics*, and in [1]) first explicitly applies vCZ to pure monochromatic situations.

17. Practically all quantitative imaging involved view ports such that θ_{Obs} =8-9^{o}(e.g. Fig 1). This allowed for high resolution with reasonable f# lenses, yet angles small with respect to aberrations (Cosθ=1) and large with respect to Rayleigh. Available view port geometry accessed only "P" polarization scatter (the LIGO beams are horizontally polarized). A full vector description of scatter (from even statistically azimuthally isotropic surfaces) then predicts azimuthal dependence (but only in brightness, not speckle character, and no more than a 1% correction from scalar for θ_{Obs} discussed here).

18. H. Yamamoto, LIGO-T070082-03-E; W. Kells, LIGO-T070051;

19. Unless a single scatter source (i.e. our HR beam spot) contributes, the distribution of image intensity will not be exponential at sufficiently low intensity (the text[1] by Goodman, **3.3**). In these experimental circumstances it is difficult to avoid secondary, contaminating, coherent [speckle] sources. Various sources of noise in the CCD recording/read out process can effectively be such a source.

20. W. Kells, LIGO-T080010-00-D.

21. J. Ohtsubo & T. Asakura, *Opt. Comm.* **14**, 30. These experiments demonstrate clearly that sufficiently un-correlated and high contrast (no specular interfering component) imaged speckle is quite independent of choice of image plane ("defocus", δf) for $\delta f/f << 1$ (but allowing $D\delta f/f >> \rho_A$). The fundamental Physics of this behavior is developed in F. Zernike, *Physica* **5**, 785 (1938) (See Ref. 1, Section 4.5).